ARKIV

Prediction of sandstone parameters from texture

Norsk Regnesentral
ANVENDT DATAFORSKNING
Norwegian Computing Center/Applied Research and Development

NOTAT/NOTE

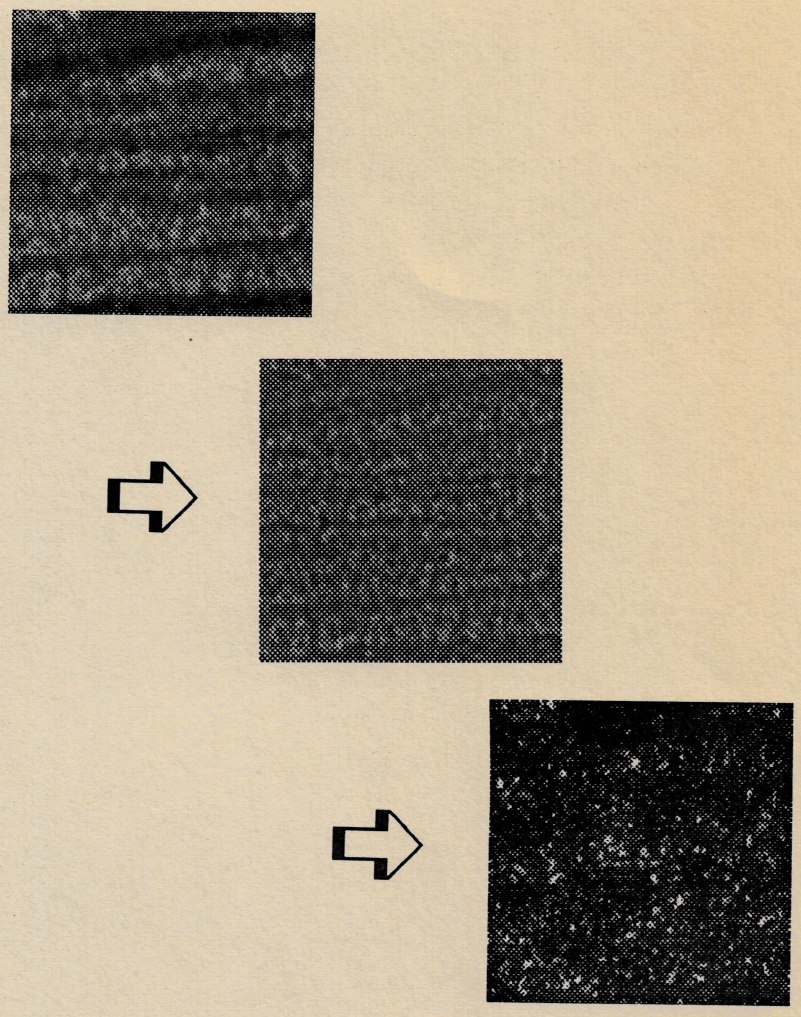

BILD/10/94

Rune Solberg
Tove Andersen
Jørn Lyseggen
Hans Koren

Oslo
September 1994

Norsk Regnesentral
ANVENDT DATAFORSKNING

NR-notat/NR-Note

Tittel/Title:
Prediction of sandstone parameters from texture

Dato/Date: September
År/Year: 1994
Notat nr:
Note no:BILD/10/94

Forfatter/Author:
Rune Solberg, Tove Andersen, Jørn Lyseggen, and Hans Koren

Sammendrag/Abstract:
This report describes an extension of the experiment "Texture analysis of sandstone surfaces" described in NR Note BILD/08/94. The objective of the study was to investigate possible textural features that can be applied to characterize different sandstone facies. A larger data set, consisting of 11 samples with known sandstone parameters and five samples with unknown parameters, was available in this experiment. The specified parameters of interest are permeability, grain size, porosity, and contents of quartz, clay, and feldspar. The textural features that showed strongest correlation were the Local GLCM features Inertia and Contrast, and the Global GLCM features Inverse Difference Moment and Inertia. The strongest correlation was found between grain size and Inertia (95\%). Some geometrical features were also extracted from segmented sandstone images, however, the correlation was not very high for any of these features. GLCM spectra were calculated by varying the distance parameter in the textural features. The spectra indicated that values in the interval 6-10 should give good discrimination between the sandstone images. Linear regression models based on the best Global and Local GLCM textural measures were calculated for the sandstone parameters, and PLS regression was calculated on a subset of the GLCM spectra by SINTEF. A comparison between the parameters for the five samples with unknown parameters after the release of these values, shows that both models predict several of the sandstone parameters fairly well.
Emneord:

Indexing terms:
Sandstone surfaces, texture analysis.
Målgruppe/Target group:

Tilgjengelighet/Availability:
Open
Prosjektdata/Project data:

Prosjektnr/Project no:

Antall sider/No of pages: 37

Satningsfelt:

Research field:

Norsk Regnesentral/Norwegian Computing Center
Gaustadalléen 23, Postboks 114 Blindern, N-0314 Oslo, Norway
Telefon 22 85 25 00, telefax 22 69 76 60

Contents

1 Introduction **4**

2 Suppression of layering **6**

2.1 Method 6

2.2 Experimental results 6

3 Textural features tested **8**

3.1 Local GLCM 8

3.1.1 Method 8

3.1.2 Experimental results 8

3.2 Global GLCM 14

3.2.1 Method 14

3.2.2 Experimental results 17

3.3 GLCM Spectrum 17

3.3.1 Method 20

3.3.2 Experimental results 20

4 Geometrical features tested **25**

4.1 Method 25

4.1.1 Experimental results 25

5 Prediction of sandstone parameters **30**

6 Discussion and conclusions **35**

1 Introduction

This report describes an extension of the experiment described in [6]. The objective of the study was to investigate possible textural features that can be applied to discriminate between different sandstone facies. If such methods exist or can be developed, the best methods will be evaluated by Reslab A/S and Norsk Hydro A/S for implementation in a sandstone characterization system applied for oil-well core analysis.

Core analysis at Reslab A/S is currently done by manual inspection of digitized video images. An image is displayed on a computer screen and analysed by an operator. The operator can do some image enhancement to assist the image interpretation. If some of the interesting parameters can be determined from the texture, and/or determined spectrally from the colour image, sandstone facies characterization could be done partially automatic.

In the previous study by Koren et al. [6], images of only four sandstone facies were available. In the current experiment, a larger data set, consisting of 11 samples with known sandstone parameters and five samples with unknown parameters, was available. The objective was to determine a relationship between sandstone texture and one or more of these parameters using the 11 samples, and then predict the same parameter(s) for the rest of the samples. The specified parameters of interest are permeability, grain size, porosity, and contents of quartz, clay, and feldspar.

The data set consists of a mosaic of 4×4 subimages of sandstone facies (see Figure 1). Each image has a size of 128×128 pixels covering an area on the sample of 1.3×1.3 cm^2. The images were acquired by a camera generating three band images in red, green, and blue light with a constant illumination angle of 15°. The laboratory measurements of the sandstone parameters are given in Table 1.

Due to a strict deadline given by the organizers of this experiment, only two weeks were available to perform the work. The experiments have, therefore, been a straight-forward continuation of the experiments described in [6]. More time would have allowed us to test more methods and to perform experiments for optimizing the methods for the given task.

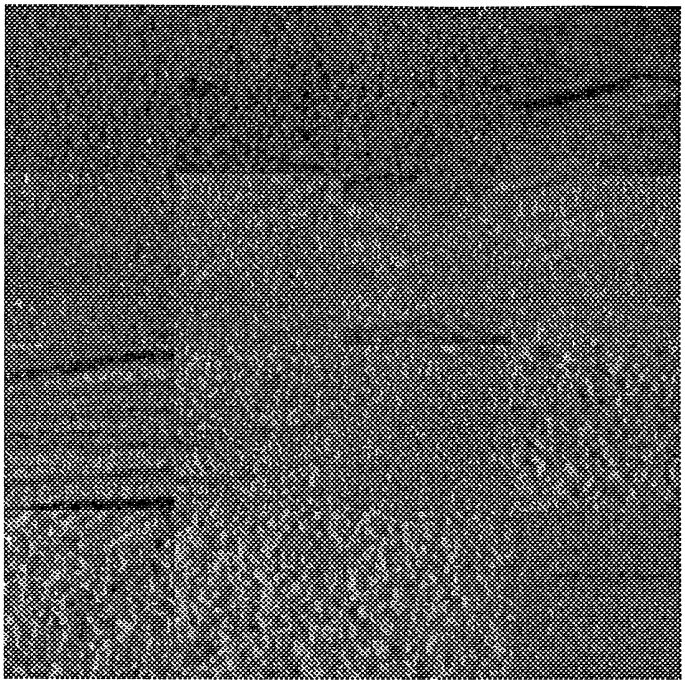

Figure 1: *Original mosaic of sandstone facies images (red band).*

No.	Permeability	Porosity	Grain size	Quartz	Clay	Feldspar
1	1.63	19.5	0.150	54	21	24
2	5.02	19.7	0.160	62	16	22
3	?	?	?	?	?	?
4	0.037	7.7	0.085	29	44	20
5	1.17	16.2	0.125	50	26	24
6	4.38	18.6	0.160	62	13	24
7	1.02	15.5	0.130	38	34	22
8	?	?	?	?	?	?
9	1.000	13.8	0.140	51	27	19
10	2.100	15.5	0.140	49	27	22
11	?	?	?	?	?	?
12	694	24.3	0.310	71	9	20
13	1660	21.7	0.360	80	7	13
14	?	?	?	?	?	?
15	2290	24.6	0.300	73	9	18
16	?	?	?	?	?	?

Table 1: *Measured parameter values for the samples in the image mosaic. Samples without given values are to be predicted. Permeability is measured in MD, porosity in percentage, grain size in millimeter, and the mineral contents in volume percentage.*

2 Suppression of layering

The previous experiment [6] showed that layering in the sandstone facies in most cases will influence much on the calculated texture. Experiments with the current data set confirmed this (see Sections 3 and 4). A method was therefore developed to suppress the layering in the facies.

2.1 Method

The idea behind the suppression algorithm proposed here is based on the fact that layering normally is present on a much larger scale in the image than the texture originating from the grainness of a sandstone surface is. In the frequency domain (e.g. in a Fourier transform of the image, see e.g. [4]) this means that the texture represents relatively high-frequent components of the transformed image, and the layering represents low-frequent components. By suppressing the low-frequency information, the layered structures should be removed.

An approach applying image transforms in the spatial domain was selected here. However, if suppression of layering is to be implemented in an operational system, a high-pass filtering approach in the Fourier domain should also be investigated before selecting a method. This means that a suitable high-pass filter should be designed and tested based on a large sandstone image data set representing the natural variations of layering.

In brief, the method works as follows:

1. Calculate the mean pixel value of the image
2. Make a mask defining the bright areas in the image (values above the mean)
3. Calculate the mean value of the part of the image with the brightest areas using the mask
4. Low-pass filter the original image by a mean filter to determine the layered structures
5. Apply the low-pass filtered image and the mean value of the bright part of the image to steer a process "lifting" the gray level in the layers.

2.2 Experimental results

Figure 2 shows the result of applying the method on sample no. three from the previous experiment [6]. A 9×9 mean filter was applied. The dominating dark layers are brightened and the corresponding structures are barely visible.

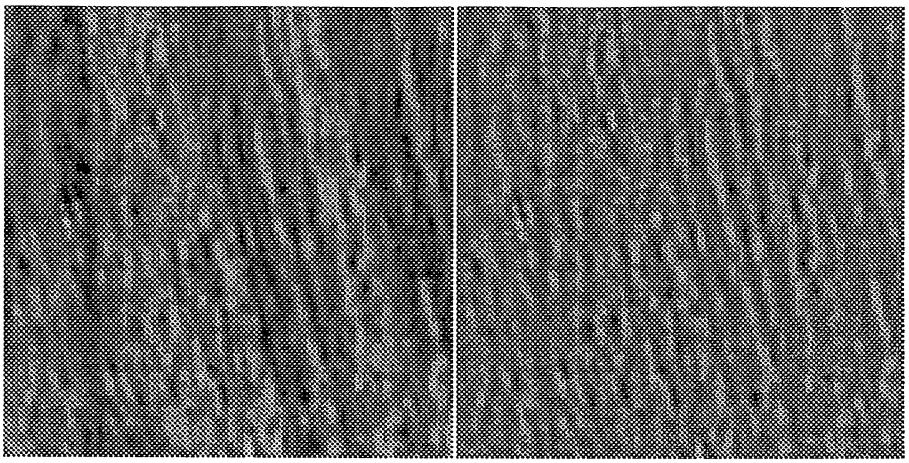

Figure 2: *Original layered image (left) and the layer-suppressed version (right). The original is sample number 3 in the previous experiment (Koren,1994).*

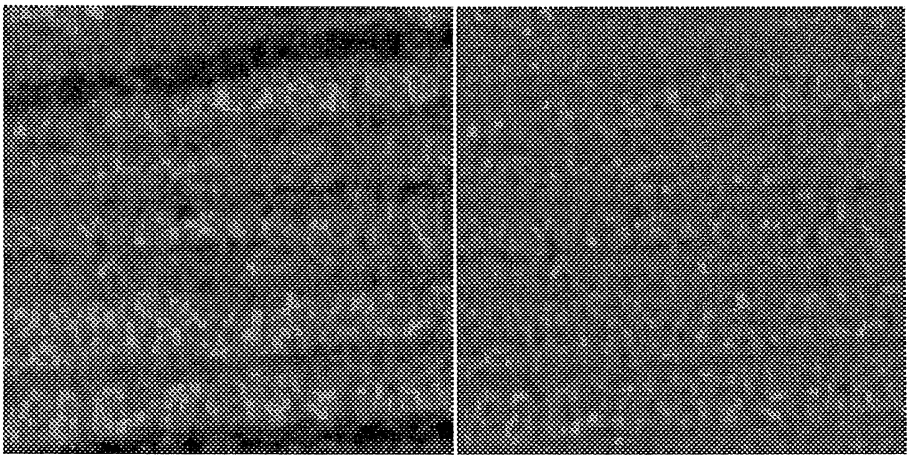

Figure 3: *Original layered image (left) and the layer-suppressed version (right). The original is sample number 9 in the current experiment.*

A corresponding experiment was performed for sample no. 9 in the current data set (Figure 3). The image is composed of six medium dark layers and two very dark layers. All the layers have been greatly suppressed, and the texture has been preserved. Note that the texture is different within and outside the previously dark layers. This is due to the smoothness of the clay-rich layers (smaller grain size).

The results of applying the method as preprocessing before texture analysis are demonstrated in Sections 3 and 4.

3 Textural features tested

Two versions of textural measures based on Gray Level Coocurrence Matrices (GLCM) have been tested. The first version was described in [6]. The second version is a modification of the first, calculating texture in one direction only. Since the image texture can be assumed to be isotropic, this simplification will make processing faster without loosing important information. Applying the latter method, texture spectra have been calculated by varying the distance parameter. Such spectra can be used to determine the optimum value of the parameter. The methods described as *Texture from region statistics* in [6] have also been tested here.

3.1 Local GLCM

3.1.1 Method

The method is described in [6]. We will only briefly describe it here: The textural features are derived from the so-called Gray Level Coocurrence Matrix (GLCM) [5]. The matrix P is a $n \times n$ matrix, where n is the number of gray levels in the image. A matrix element $P_d^\theta(i,j)$ is given by the relative frequency of a pixel pair with gray levels i and j, respectively, at a distance of d pixels, and at an angular direction θ. Typical values of θ are 0, 45, 90 and 135 degrees. We have applied the mean value of these four directions. A GLCM may be calculated for the whole image ("global GLCM"), or in a repetitive manner for a moving window in the image ("local GLCM"). In the first case, the result will be a single textural feature value, and in the second case the result will be a new image where each pixel represents the local texture. Haralick et al. [5] have proposed a set of 14 textural features that can be derived from a GLCM. Some other features have been proposed by Conners et al. [3].

3.1.2 Experimental results

In the study described in [6], we found a certain correlation between some textural features and porosity and contents of quartz in the sandstone samples. In the previous study, based on only four samples, there was a positive correlation between the porosity and the contents of quartz. These two properties seemed not to be correlated to the grain size. During the previous study we found no good correlations between the textural feature measures and the grain size.

In the new set of samples, there seems to be some positive correlation between grain size, contents of quartz and porosity, and even the permeability. The values of these properties are shown in the Figures 4, 5, 6, and 7. The values of the contents of clay and feldspar are shown in Figures 8 end 9.

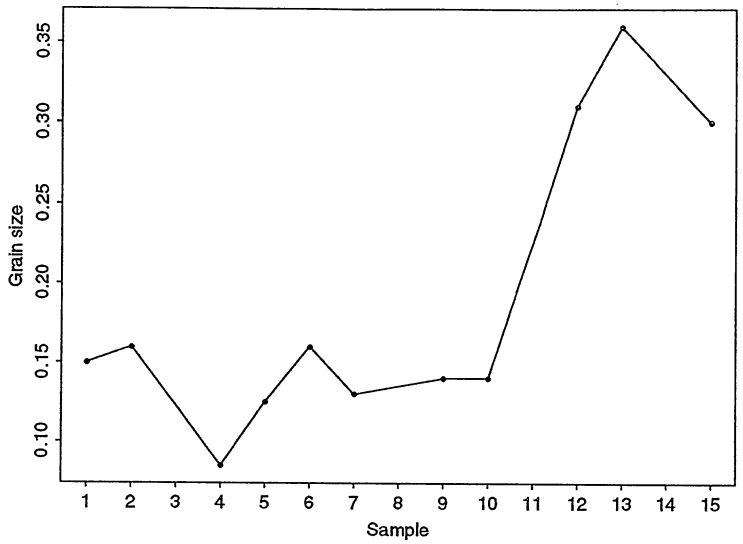

Figure 4: *Grain size of known samples.*

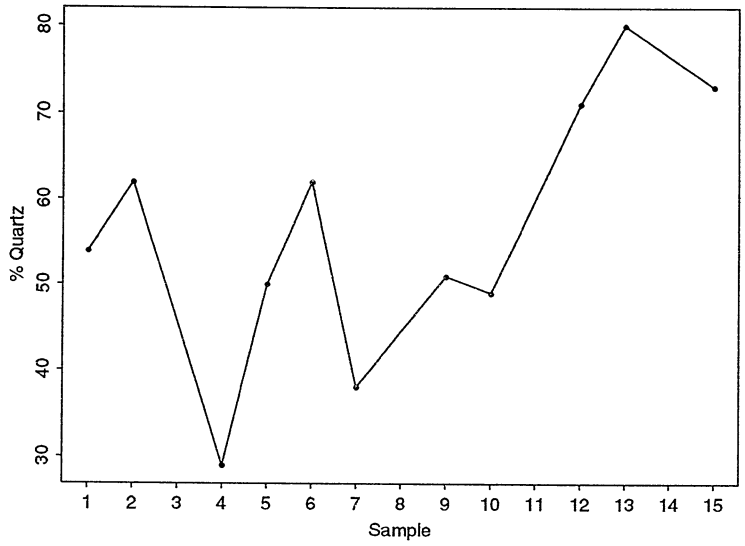

Figure 5: *Quartz contents of known samples.*

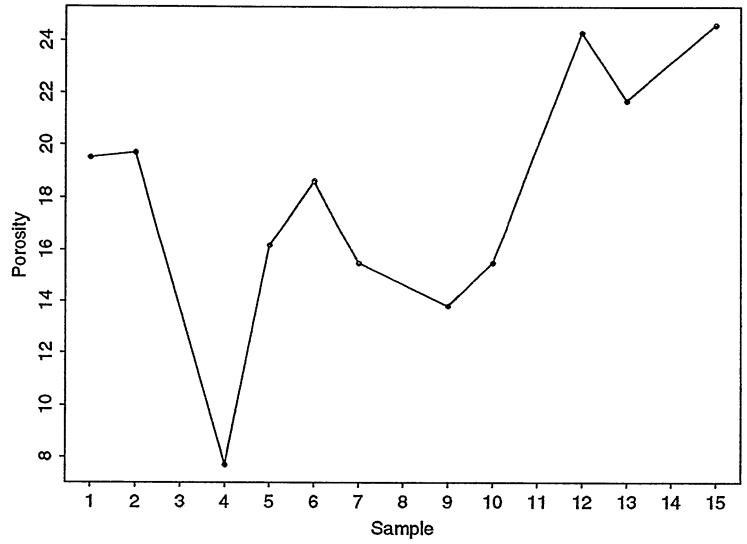

Figure 6: *Porosity of known samples.*

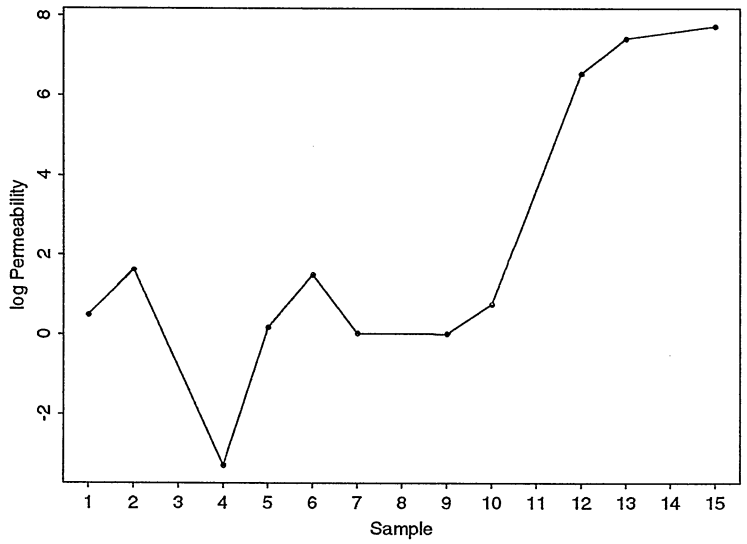

Figure 7: *Permeability (logarithmic value) of known samples.*

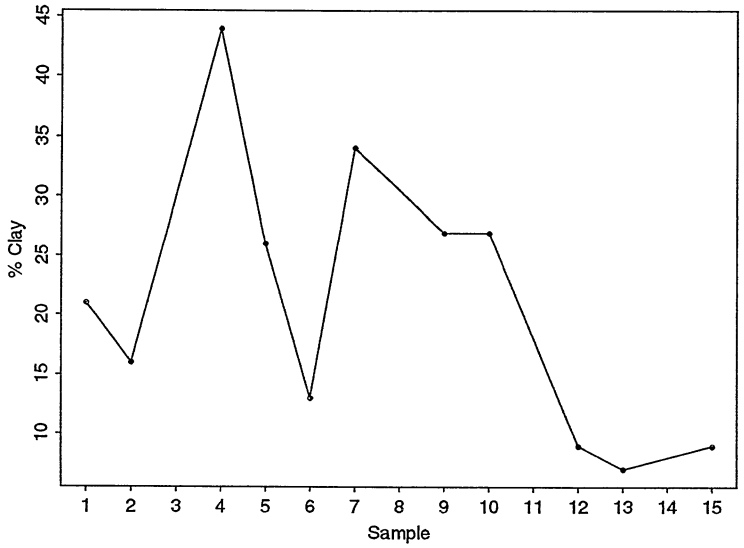

Figure 8: *Clay contents of known samples.*

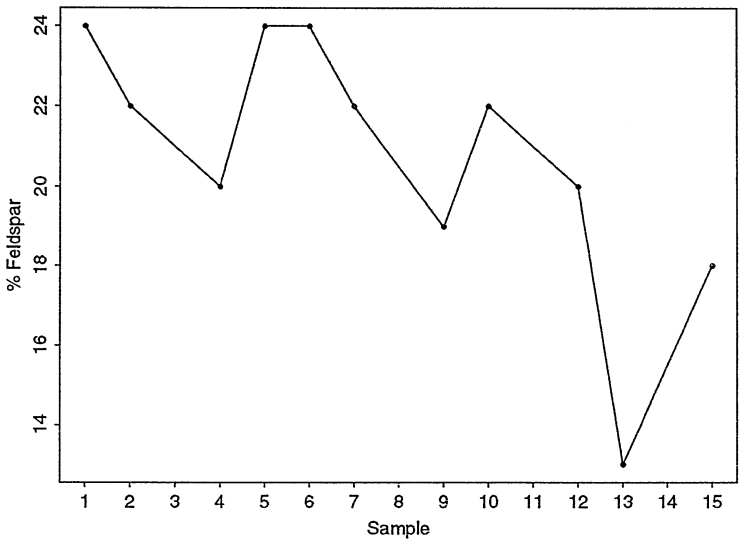

Figure 9: *Feldspar contents of known samples.*

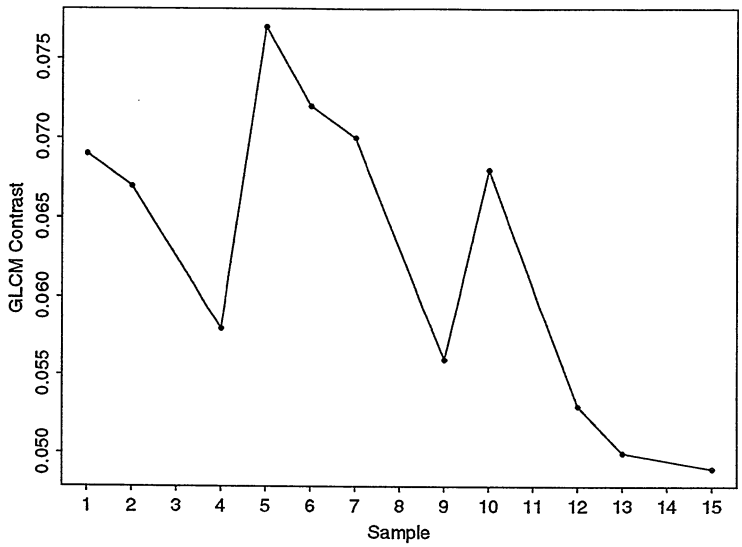

Figure 10: *GLCM Contrast of original images with known properties.*

Textural measures were calculated for the 16 images in the same way as described in [6]. We first tested the features that gave the best correlation of porosity and contents of quartz in the previous study. These were the mean gray value, GLCM Correlation, Contrast and Homogeneity. These measures showed little correlation with the properties of the new sandstone samples. Next, we tried all the textural measures used in the previous study, and now other features gave the best results. The highest correlations were found for grain size.

The GLCM measures Contrast and Inertia gave the best results. The calculations were performed with 16 gray levels and a window of 15×15 pixels. A distance of $d = 1$ pixel was used, and the mean of four directions was calculated. When calculating the features for the original images, the correlation was not so good for the images with marked layered structures. These are images no. 4, 7 and 9. After preprocessing by layer suppression, described in Section 2, higher correlations were achieved.

The differences between the calculations with and without layer suppression are shown in Figures 10 and 11 for the samples with known properties. We can see that the values for the layered images, no. 4, 7 and 9, have changed a lot relatively to the other samples.

These figures should be compared to the figures showing the known properties, Figures 4 - 9. We can see that calculating the GLCM Contrast results in a certain correlation with some of the properties, especially grain size and permeability. Be aware that the correlation is negative. The calculations on layer suppressed images give much better correlations than using the original images.

The correlations between the GLCM Contrast measure calculated for the layer suppressed

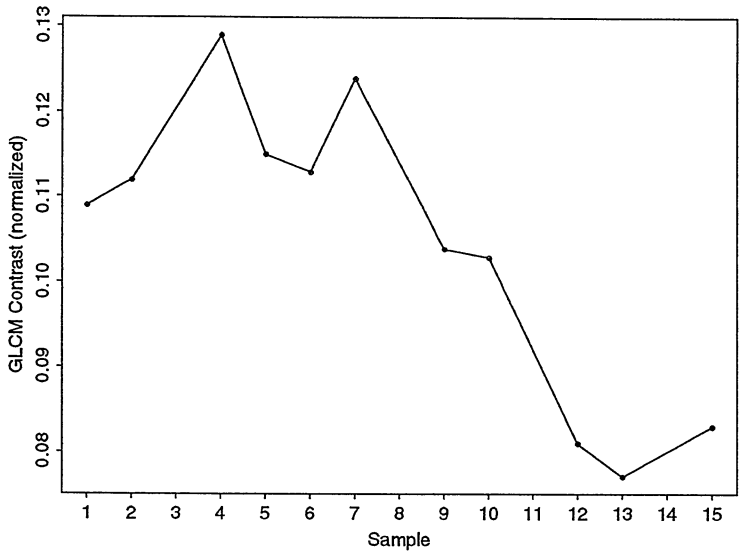

Figure 11: *GLCM Contrast for layer suppressed images with known properties.*

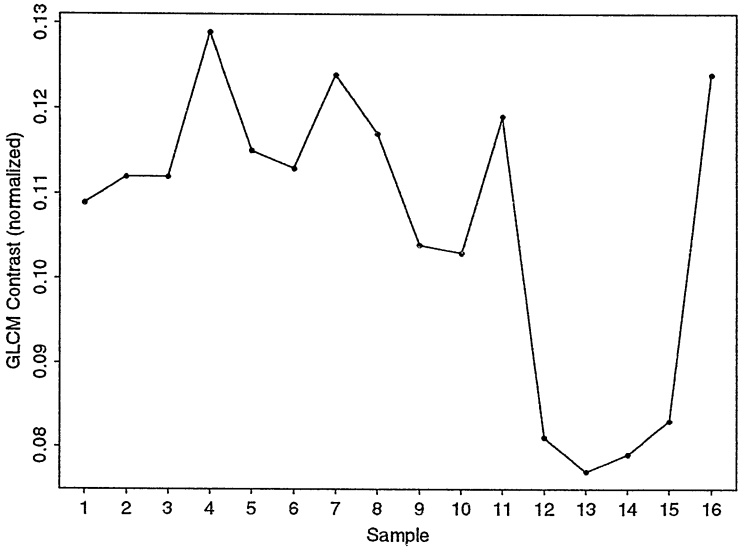

Figure 12: *GLCM Contrast for layer suppressed images, all samples.*

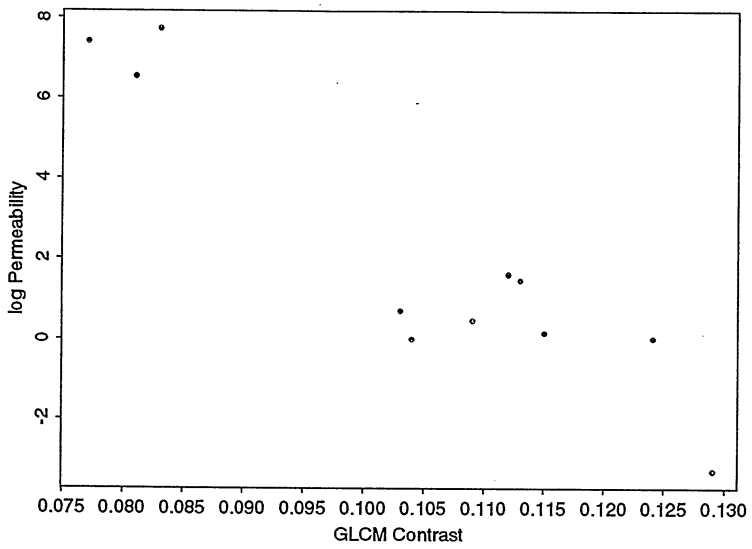

Figure 13: *The logarithm of permeability as a function of GLCM Contrast.*

images and the various properties are shown in Figures 13 - 18.

A certain correlation is found with most of the properties. The best results are achieved for grain size and permeability. Contents of quartz and clay are also well correlated with the GLCM contrast. Less correlation is found for the porosity and the contents of feldspar.

Calculation of the correlation and predictions of the values for the samples no. 3, 8, 11 14 and 16 were performed for the best correlated properties, grain size and permeability. The results are found in Section 5.

3.2 Global GLCM

In this experiment, we have increased the dimensionality of the GLCM to a 256×256 matrix and calculated textural measures globally. An efficient method for generation of the 256 × 256 GLCM was implemented. This method utilizes the isotropic property of the sandstone samples and lends itself to efficient real time computation.

3.2.1 Method

The basic approach in this method is to consider an image as a 1-D data array. This is valid since the sandstones are isotropic. GLCM elements are then calculated by considering pixels on the same scan line. Since this method only requires one scan line at a time, the GLCM matrix can, in a real-time system, be generated concurrently with the data acquisition, something which would greatly increase inspection speed.

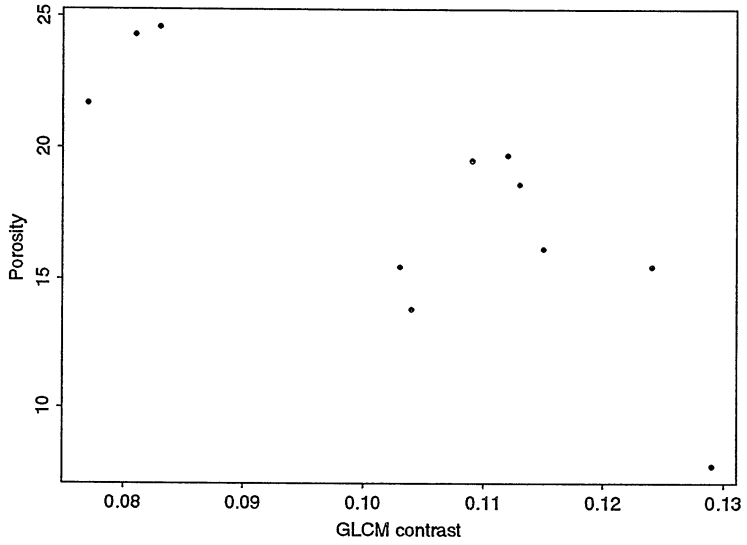

Figure 14: *Porosity as a function of GLCM Contrast.*

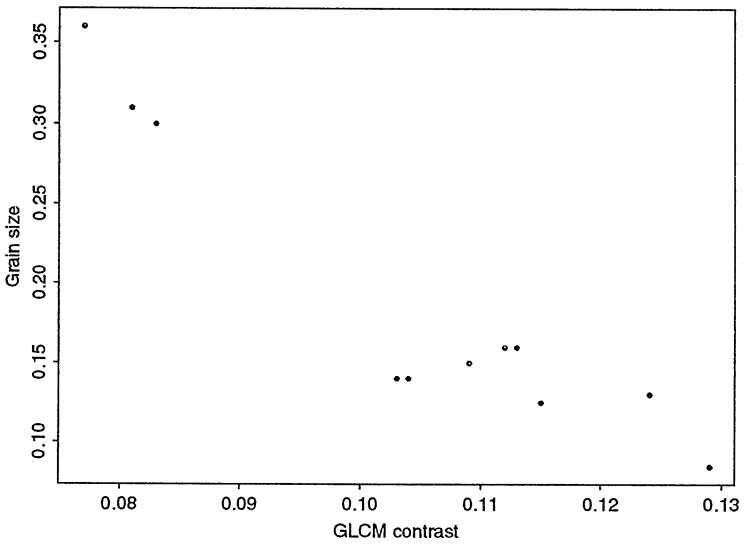

Figure 15: *Grain size as a function of GLCM Contrast.*

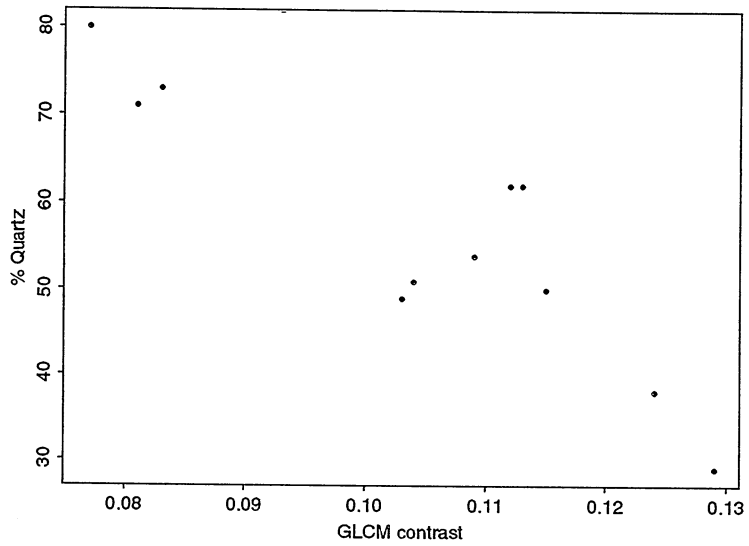

Figure 16: *Quartz contents as a function of GLCM contrast.*

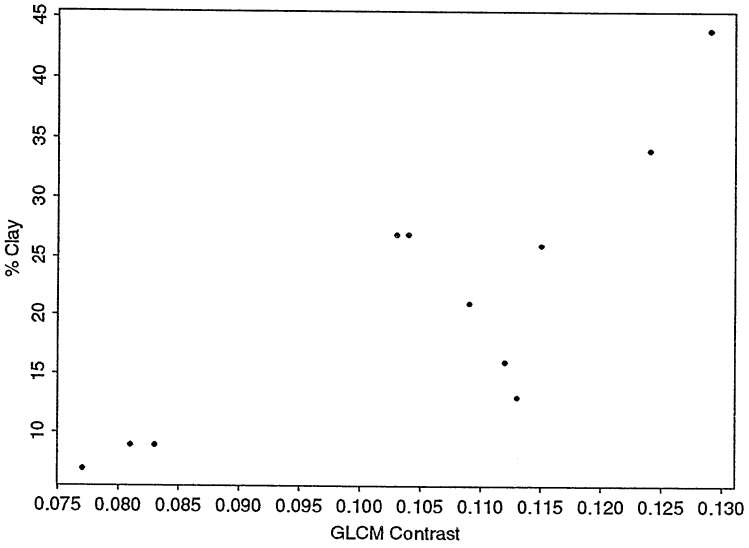

Figure 17: *Clay contents as a function of GLCM contrast.*

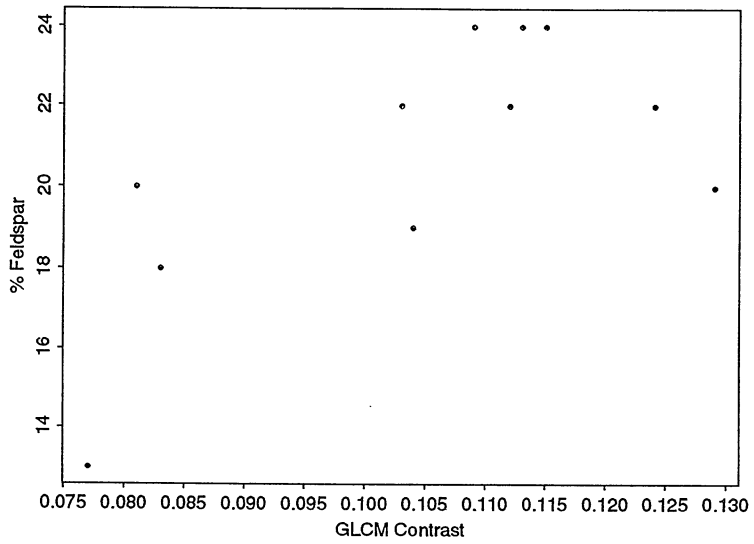

Figure 18: *Feldspar contents as a function of GLCM contrast.*

Another difference between the GLCM reported in the previous section and this version is that the 16×16 GLCM were calculated locally within a moving window, whereas this GLCM are calculated globally for each sandstone image. The advantage of a global implementation is that it is more efficient and that it is less sensitive to local variations.

The features calculated based on the 256×256 GLCM are the same as those reported on for the 16×16 GLCM.

3.2.2 Experimental results

When plotting the GLCM features for fixed values larger than 1, we found a strong relationship between several of our texture features and the sandstone properties. This was particularly true for grain size, clay, quartz, and porosity. Two illustration of these relationships are shown in Figures 19-20. Calculated correlations are found in Section 5.

3.3 GLCM Spectrum

Earlier attempts to correlate texture and the sand stone properties were performed using individual features at a fixed distance. Inspired by the work of [2], our new attempt here is to study the change of such individual features as the distance between the pixels of interest is varied. This gives us important information about the change in spatial dependencies within a texture pattern.

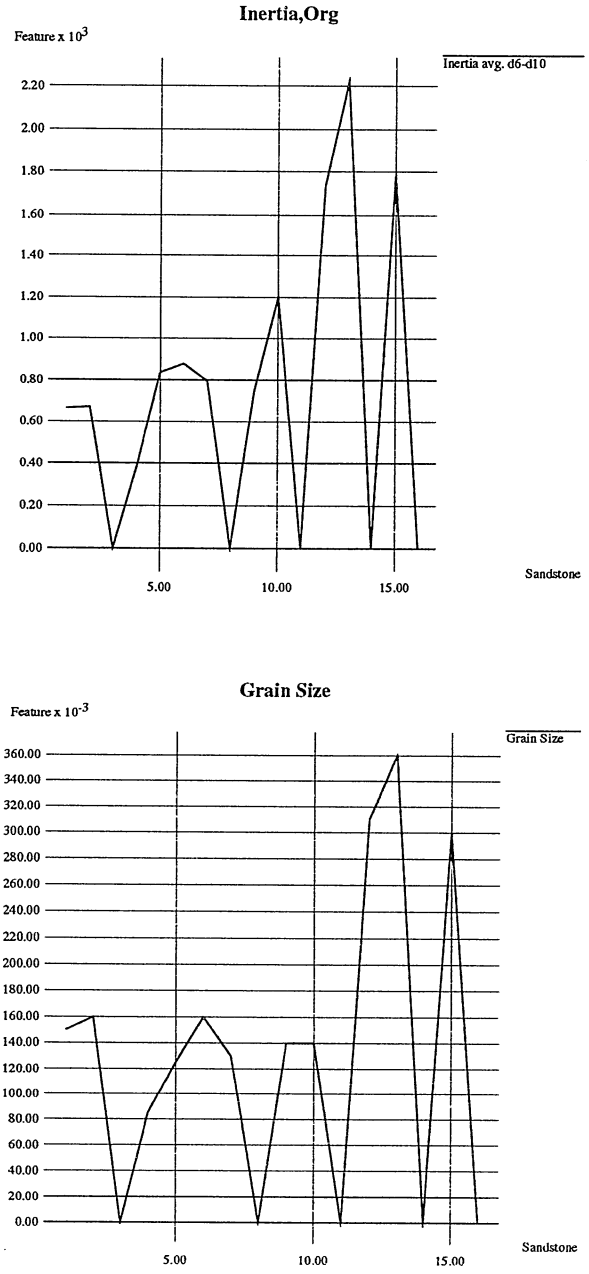

Figure 19: *The graphs show the strong relationship between grain size and inertia. Feature values for sandstones with unknown properties are set to zero.*

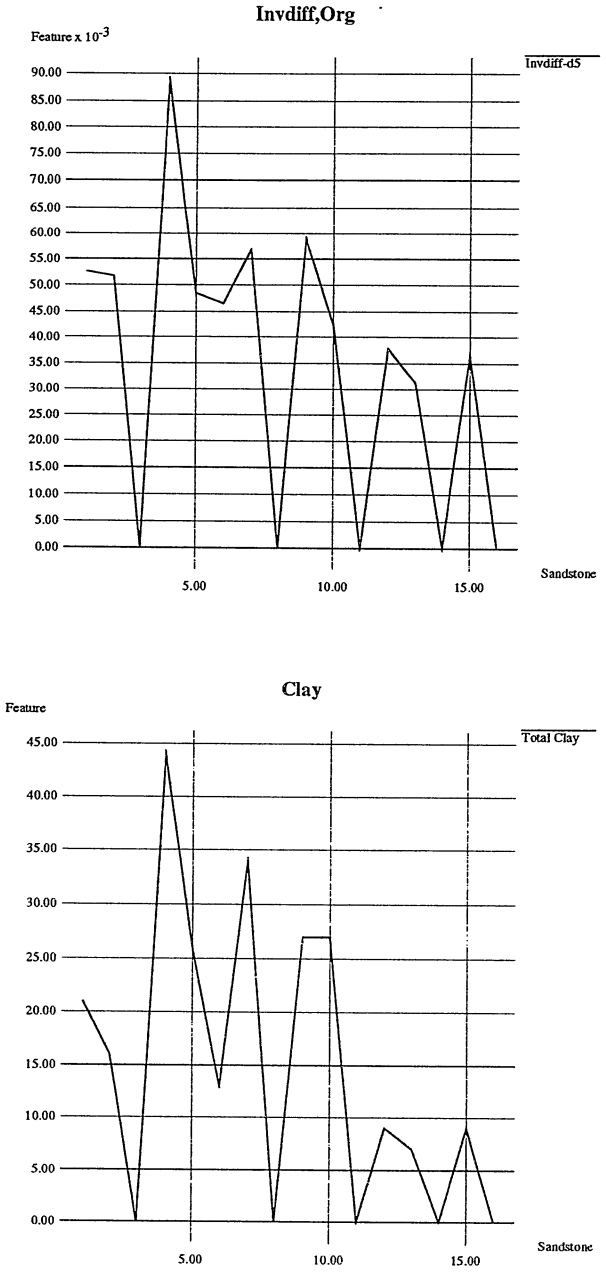

Figure 20: *The graphs show the strong relationship between clay and inverse difference moment. Feature values for sandstones with unknown properties are set to zero.*

3.3.1 Method

Six GLCM features were calculated and plotted as functions of the distance between the pixels. These were Absolute Difference Moment, Inverse Different Moment, Inertia, Angular Second Moment, Entropy, and Autocorrelation. Absolute Difference Moment (ADM) and Autocorrelation (AC) are defined as

$$f_{ADM} = \sum_i \sum_j |i-j| p(i,j) \tag{1}$$

$$f_{AC} = \sum_i \sum_j ijp(i,j). \tag{2}$$

The other features were defined in [6].

The Absolute Difference Moment is related to Inertia and Inverse Difference, all being functions of the difference $(i-j)$. The Inverse Difference has good discriminatory capacity in the lower contrast range whereas Inertia is best for high contrasts. The Absolute Difference works equally well for all contrasts without being tailored to a particular contrast range.

The Autocorrelation is a scaled and shifted version of the Correlation feature discussed in previous report. These two features have the same information contents, however, Autocorrelation was preferred over Correlation because of less computational cost.

3.3.2 Experimental results

When plotting the different GLCM features as functions of distances we observed two :

1) The functions vary in general considerably for distances less than 6-7 and then stabilize.

2) The features discriminated in general very well between the 16 different sandstones shown in Figures 22 and 24.

The first observation justifies a study of the GLCM features for higher distances than 1.

The second observation is very encouraging. To correlate the sandstone properties with our features, it is necessary that our features are able to discriminate between the different sandstones, and this was evident in most of our GLCM feature plots.

An interesting observation is that the layer suppression clearly stabilized several of the features for stones with clear directional information. This can be seen clearly in the plots of Entropy and ASM. The plots for the original image 4 and 9, which are the images with the strongest information contents, are not stabilizing for large differences. This does not

match with an isotropic coherent assumption, but when plotting the corresponding values for the layer suppressed images, all curves are stabilizing for larger distances.

Four examples of 256×256 GLCM features are shown in Figures 22 to 24. Within each graph there are 16 curves, one for each sandstone. The information contents varies in the lower distances and stabilizes as the distance increases. The plots also shows that the GLCM features can discriminate between all 16 sandstones.

The plots in Figures 25 and 26 show the effect of the layer suppression. In Figure 25, one can see two ramp-like curves which are crossing the others. These correspond to sandstone 4 and 9 which are the samples with the strongest directional information contents. Directional information violates the isotropic assumption made in calculating the GLCM features, but is compensated for by the layer suppression method. In Figure 26, one can see the effect of the layer suppression. The two deviating plots have now been stabilized for larger distances.

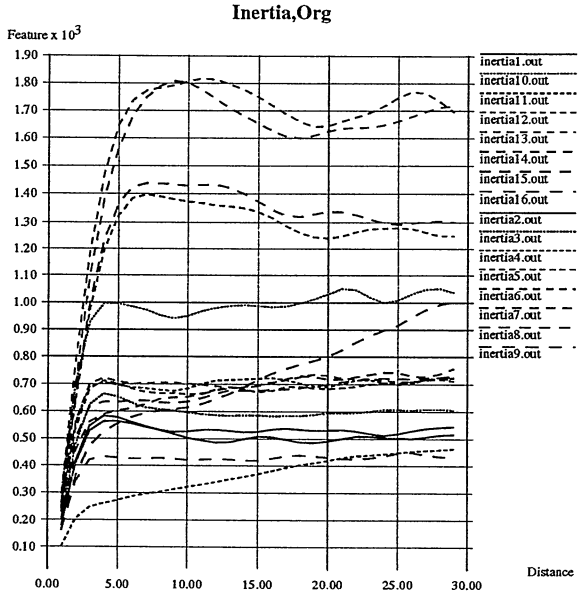

Figure 21: *GLCM spectrum for Autocorrelation from original image.*

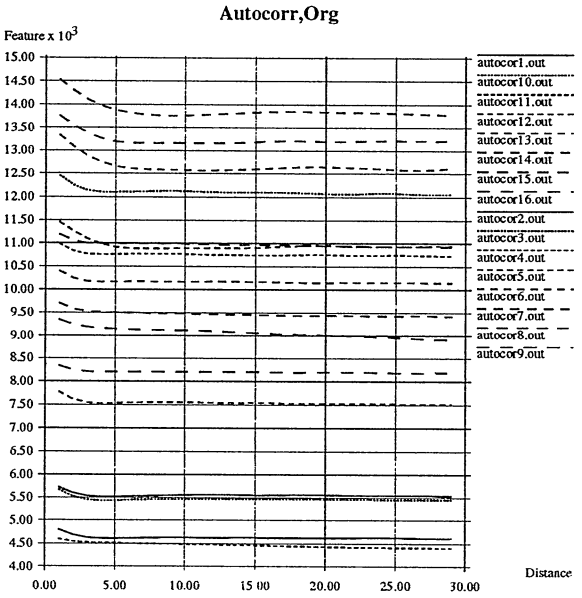

Figure 22: *GLCM spectrum for Inverse Difference Moment from original image.*

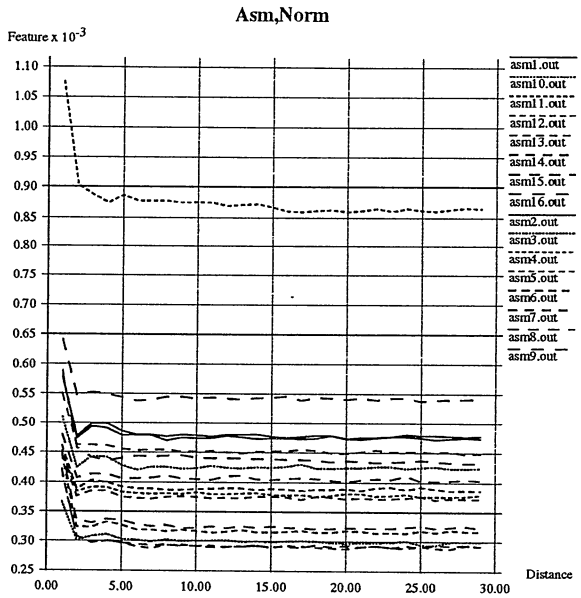

Figure 23: *GLCM spectrum for ASM from layer suppressed image.*

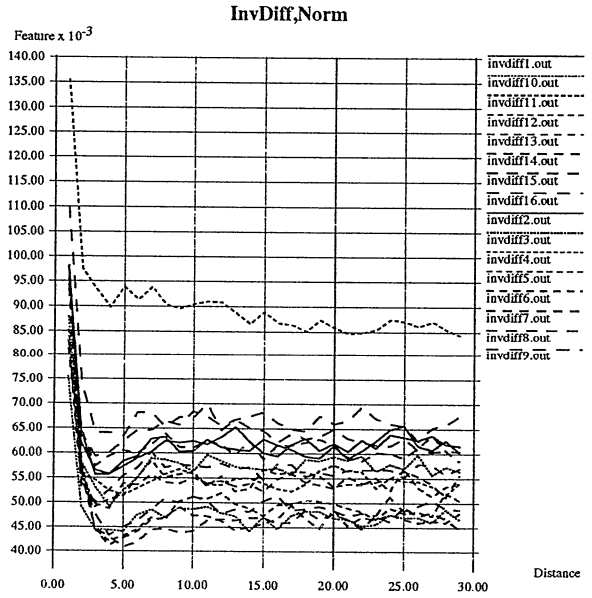

Figure 24: *GLCM spectrum for Inverse Difference Moment from layer suppressed image.*

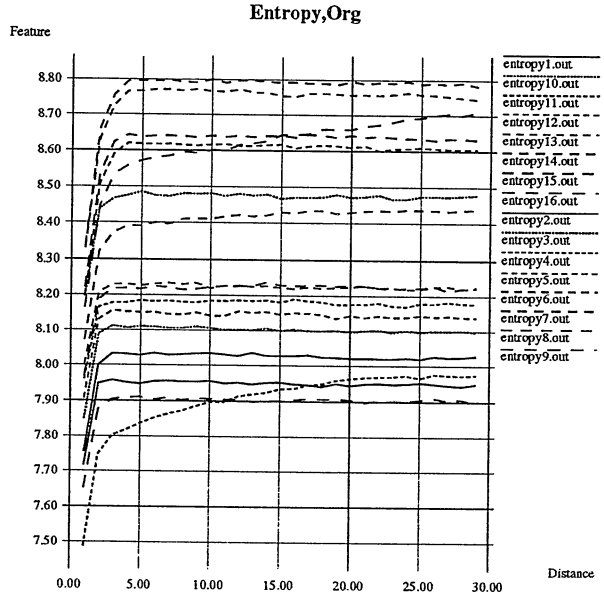

Figure 25: *GLCM spectrum for Entropy from original image.*

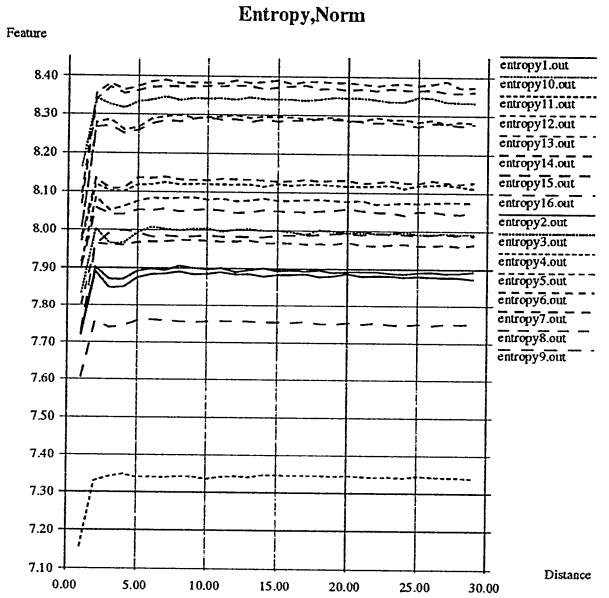

Figure 26: *GLCM spectrum for Entropy from normalized image.*

4 Geometrical features tested

A method based on texture from region statistics was tested in [6]. The results there indicated that mean size and standard deviation of the texture regions were correlated to some sandstone parameters. We have extended that experiment here by performing region analysis on a segmented version of the original image.

4.1 Method

The original image has 256 gray levels. The segmentation applied here divided the gray level scale into a specified number of equal intervals. Each pixel was then labeled according to the corresponding interval. Since the pixel values are spatially correlated, local groups of pixels make up regions. The number of regions depends on the degree of spatial correlation.

Parameters from regions from only a part of the gray scale might be correlated with the sandstone parameters. The method, therefore, applies a user-specified threshold value defining which part of the gray scale to generate regions from.

The segmented image is then analysed by generating a set of geometrical measurements. These are mean size, A, mean perimeter, P, and mean complexity, P^2/A. The list of geometrical features can easily be extended.

4.1.1 Experimental results

Calculations were performed for different gray scale intervals between 10 and 50, and various thresholds.

The best results were achieved by segmenting the layer-suppressed images with a gray level interval of 50, and an upper threshold of 100. In this case, only the two darkest sets of regions were used in the calculations.

The results are shown in Figures 27, 28, and 29. The grain size, the contents of quartz, and the porosity are shown as a function of the mean area of the segmented regions. A certain correlation may be observed, but the results are not too promising. For the mean perimeter, similar or better results were found, as shown in figures 30 and 31.

The same calculations were performed on the data set used in [6]. The images were layer suppressed before the segmentation. The results are shown in Figures 32, 33, and 34.

With this small data set of four samples, very good correlation is found for the porosity and the contents of quartz, but not for the grain size.

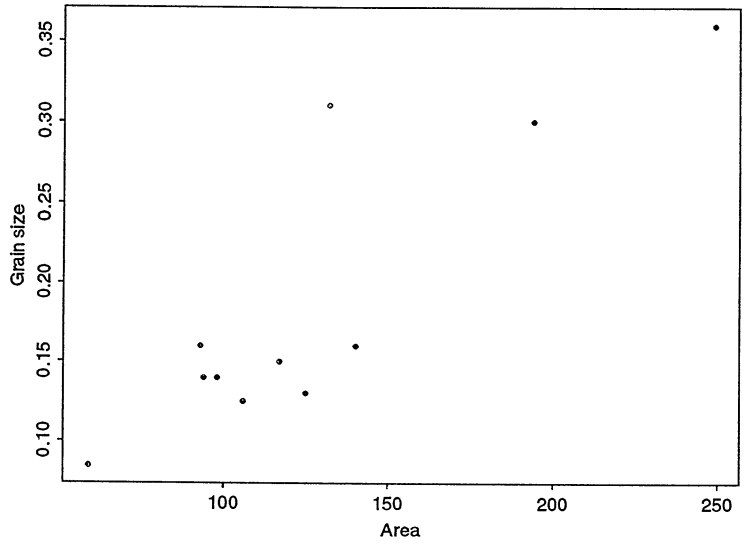

Figure 27: *Grain size as a function of mean region area.*

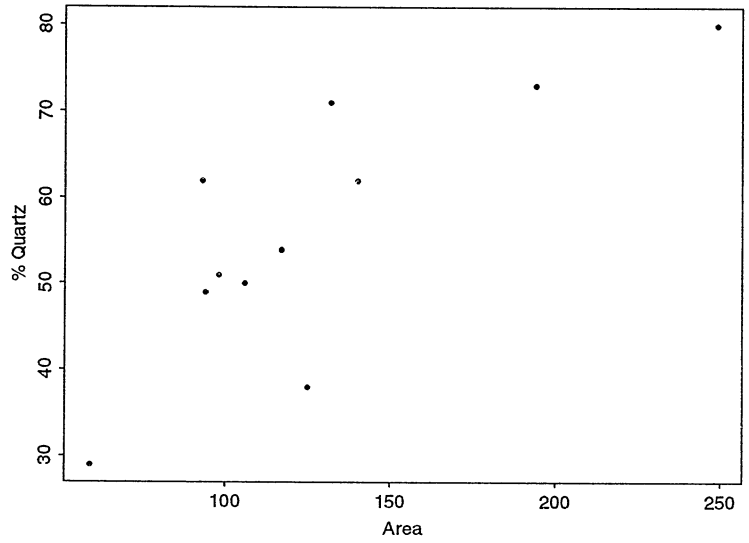

Figure 28: *Quartz contents as a function of mean region area.*

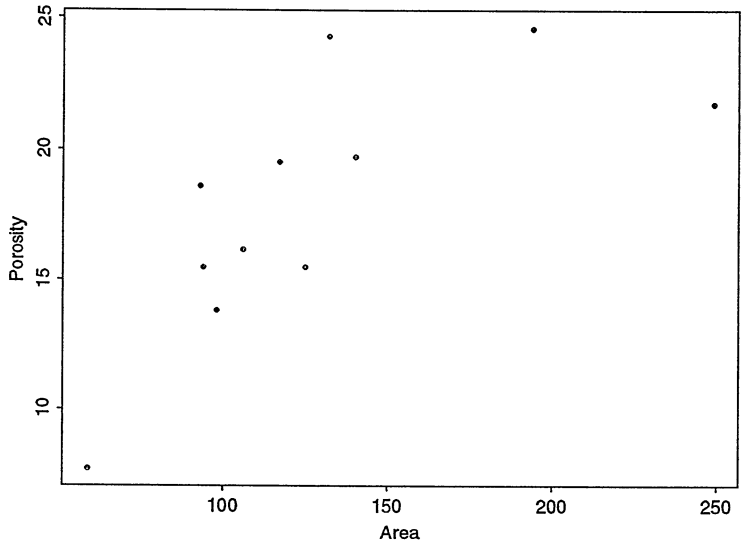

Figure 29: *Porosity as a function of mean region area.*

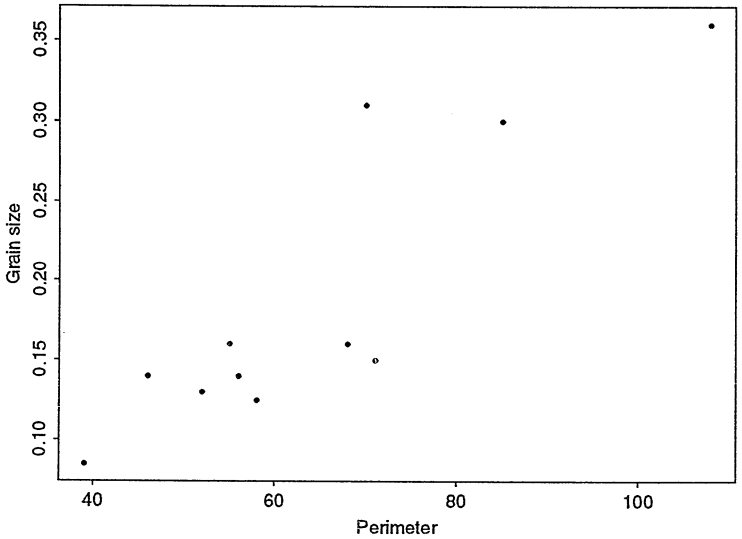

Figure 30: *Grain size as a function of mean region perimeter.*

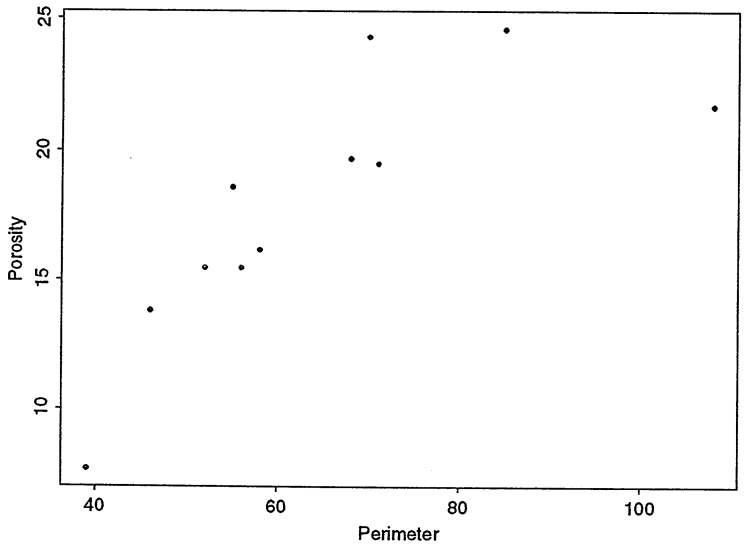

Figure 31: *Porosity as a function of mean region perimeter.*

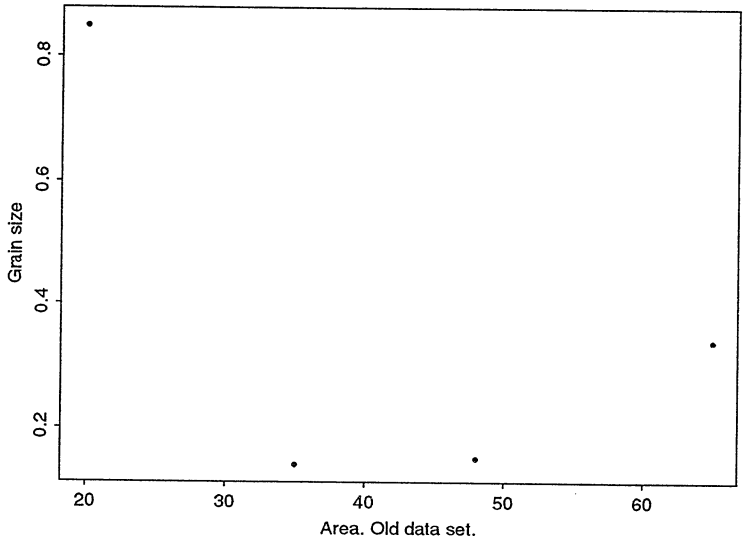

Figure 32: *Grain size as a function of mean region area. Old data set.*

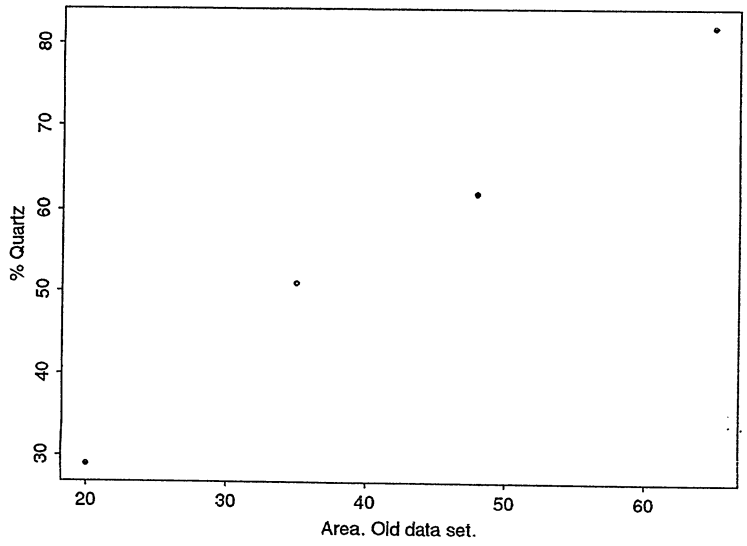

Figure 33: *Quartz contents as a function of mean region area. Old data set.*

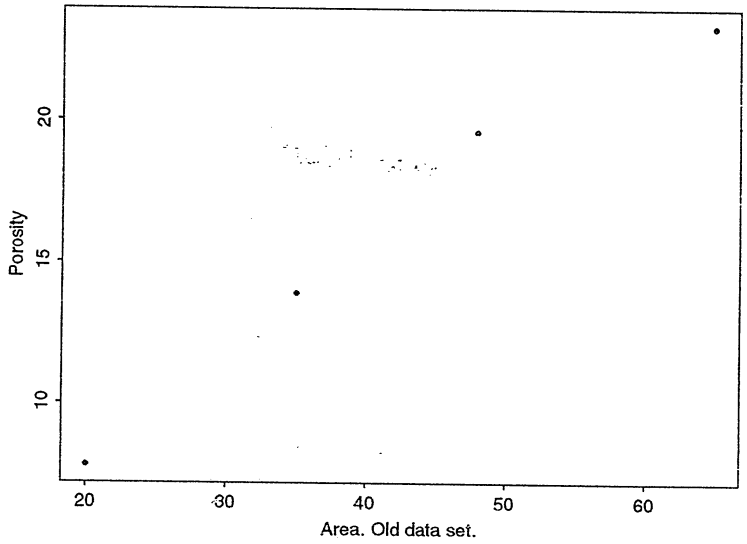

Figure 34: *Porosity as a function of mean region area. Old data set.*

5 Prediction of sandstone parameters

Linear regression models based on the texture measures (Absolute Difference, Angular Second Moment, Autocorrelation, Entropy, Inertia, Inverse Difference Moment) are calculated for the physical quantities. Due to sparse data, only a few texture measures should be used in the regression model. For each physical quantity, the most explanatory variables are selected by considering the correlation between the quantity and the texture measures. If there is a lack of correlation between the quantity and the texture measures, transformations of the texture measures is tested.

Another approach to find the most important texture measure is to use a stepwise regression method. Here the Efroymson method is used. The method is similar to forward selection with an important exception: when each new texture measure is added to the equation, partial correlations are considered to see if any of the present texture measures should be excluded. As input to Efroymson, only the most correlated pixel distance for each texture measure is used.

All regression equations are obtained by using the least squares method. The regression equations are used to predict the values of the physical quantities for the unknown samples.

The correlation between the physical quantities and the texture measures are shown in Table 7-11. The most correlated texture measure is used to construct a regression model. In some cases more than one texture measure are used in the regression equation. It is therefore important to notice that when the texture measures are highly correlated, this will often not give better prediction, only more variance. The proposed prediction models and the predictions are given in Tables 2-6. To evaluate the models the standard deviation as well as the squared multiple correlation coefficient, R^2, are provided. However, the commonly used residual estimate for R^2 is biased, therefore the leave-one-out cross-validated estimate is calculated in addition.

Model: grain =	st.dev	R^2	R^2_{cross}	pr. 3	pr. 8	pr. 11	pr. 14	pr. 16
0.0256 + 0.000149*inertia6.10	0.029	0.96	0.90	0.139	0.144	0.153	0.355	0.105
0.104 + 5.63e-08*inertia6.10^2	0.028	0.97	0.88	0.137	0.139	0.145	0.378	0.120
0.0683 + 0.000198*inertia6.10 -1.0204e-05*autocor1 (*)	0.023	0.98	0.92	0.162	0.111	0.125	0.357	0.089

Table 2: The proposed models for grain size and predictions for the five unknown observations. The model selected by Efroymson is marked (*).

Following the analysis presented previously, we calculated an additional feature: GLCM contrast.

The correlation between the GLCM contrast and the grain size is calculated to -0.95.

A prediction model is constructed based on linear regression. The predicted values for the

grain size are shown in table 12. These values are predicted from the calculations of GLCM contrast for all 16 samples shown in figure 12.

The correlation between the GLCM Contrast and the logarithm of the permeability is calculated to -0.94.

A prediction model for the logarithm of the permeability is constructed based on linear regression. The predicted values for the permeability are shown in table 13.

Model: feldspar =	st.dev	R^2	R^2_{cross}	pr. 3	pr. 8	pr. 11	pr. 14	pr. 16
-15.41 +2.36*absdiff6.10+ 12310.49*asm.6.10 - 0.0319*inertia6.10 (*)	1.20	0.99	0.78	23.6	23.1	23.8	15.0	23.6
22.36 - 3.74e-13*inertia6.10^4	1.74	0.98	0.72	22.2	22.2	22.2	13.5	22.3

Table 3: The proposed models for feldspar and predictions for the five unknown observations. The model selected by Efroymson is marked (*).

Model: clay =	st.dev	R^2	R^2_{cross}	pr. 3	pr. 8	pr. 11	pr. 14	pr. 16
60.699 - 1.834*absdiff.4	7.13	0.84	0.61	23.5	24.6	22.7	6.9	30.5
41.030 - 0.0247*inertia.4	7.73	0.82	0.53	24.7	25.4	23.6	6.9	30.3
-11.771 + 656.971*invdiff.5 (*)	6.11	0.88	0.70	20.5	20.2	19.8	10.1	27.2

Table 4: The proposed models for clay and predictions for the five unknown observations. The model selected by Efroymson is marked (*).

Model: quarts =	st.dev	R^2	R^2_{cross}	pr. 3	pr. 8	pr. 11	pr. 14	pr. 16
98.88696 -849.5829*invdiff.5	8.185	0.95	0.60	57.1	57.6	58.0	70.6	48.5
6.145 + 2.274*absdiff.5 (*)	8.342	0.95	0.70	51.9	51.1	53.2	77.4	43.5
55.668 -475.310*invdiff.5+ 1.109*abs.diff.5	8.163	0.96	0.55	54.7	54.5	55.8	74.6	45.7

Table 5: The proposed models for quarts and predictions for the five unknown observations. The model selected by Efroymson is marked (*).

Model: por =	st.dev	R^2	R^2_{cross}	pr. 3	pr. 8	pr. 11	pr. 14	pr. 16
31.824 -277.243*invdiff.5 (*)	2.541	0.96	0.73	18.20	18.34	18.48	22.60	15.37

Table 6: The proposed model for porosity and predictions for the five unknown observations. This is the model selected by Efroymson.

pixeldiff	absdiff	asm	autocor	entropy	inertia	invdiff
1	0.476	-0.599	0.695	0.675	0.588	-0.280
2	0.683	-0.674	0.692	0.725	0.739	-0.564
3	0.815	-0.694	0.684	0.743	0.857	-0.681
4	0.881	-0.702	0.677	0.749	0.914	-0.740
5	0.915	-0.694	0.671	0.740	0.940	-0.757
6-10	0.932	-0.697	0.668	0.734	0.952	-0.812

Table 7: The correlation between grain size and the six texture measures for different pixel difference. The correlation between grain and inertia.6-10 is largest. But also the correlation between grain and absdiff.6-10 is large.

pixeldiff	absdiff	asm	autocor	entropy	inertia	invdiff
1	-0.057	0.395	-0.513	-0.514	-0.231	-0.193
2	-0.249	0.479	-0.513	-0.582	-0.381	0.029
3	-0.404	0.544	-0.508	-0.631	-0.519	0.161
4	-0.504	0.562	-0.501	-0.651	-0.606	0.240
5	-0.572	0.575	-0.495	-0.658	-0.661	0.277
6-10	-0.642	0.602	-0.490	-0.674	-0.718	0.386

Table 8: The correlation between feldspar and the six texture measures for different pixel difference. Transformations of the texture measures were done to increase the correlation. The correlation between feldspar and inertia.6-10^4 are -0.864. the above correlations.

pixeldiff	absdiff	asm	autocor	entropy	inertia	invdiff
1	-0.612	0.575	-0.552	-0.574	-0.626	0.548
2	-0.743	0.602	-0.547	-0.583	-0.718	0.738
3	-0.803	0.583	-0.540	-0.573	-0.770	0.811
4	-0.815	0.576	-0.535	-0.564	-0.779	0.836
5	-0.811	0.559	-0.532	-0.547	-0.772	0.868
6-10	-0.783	0.539	-0.532	-0.528	-0.750	0.834

Table 9: The correlation between clay and the six texture measures for different pixel difference. The correlation is largest between clay and invdiff 5. There are also a large correlation between clay and absdiff 4.

pixeldiff	absdiff	asm	autocor	entropy	inertia	invdiff
1	0.584	-0.599	0.590	0.617	0.627	0.584
2	0.740	-0.637	0.585	0.637	0.739	0.740
3	0.821	-0.630	0.578	0.636	0.810	0.821
4	0.849	-0.626	0.572	0.630	0.832	0.849
5	0.854	-0.612	0.568	0.615	0.834	0.854
6-10	0.838	-0.598	0.567	0.600	0.820	0.838

Table 10: The correlation between quarts and the six texture measures for different pixel difference. The correlation is largest between quarts and invdiff 5. The correlation is also large between quarts and absdiff.

pixeldiff	absdiff	asm	autocor	entropy	inertia	invdiff
1	0.599	-0.568	0.539	0.557	0.599	-0.567
2	0.738	-0.604	0.534	0.573	0.697	-0.774
3	0.803	-0.578	0.528	0.561	0.757	-0.847
4	0.816	-0.571	0.522	0.551	0.770	-0.863
5	0.810	-0.548	0.519	0.530	0.764	-0.871
6-10	0.776	-0.529	0.519	0.510	0.736	-0.851

Table 11: The correlation between porosity and the six texture measures for different pixel difference. The correlation is largest between porosity and invdiff 5.

Model: grain size =	st.dev	R^2	pr. 3	pr. 8	pr. 11	pr. 14	pr. 16
0.731 - 5.245*contrast	0.031	0.96	0.144	0.117	0.107	0.317	0.081

Table 12: The proposed model and predictions for grain size.

Model: log permeability =	st.dev	R^2	pr. 3	pr. 8	pr. 11	pr. 14	pr. 16
9.615 - 83.323*contrast	0.571	0.99	1.92	0.73	1.10	1077	0.19

Table 13: The proposed model for the logarithm of the permeability and predictions for the permeability.

6 Discussion and conclusions

The importance of a large data set for the type of analysis represended by the previous and current experiments has been clearly demonstrated. The results of the experiments in [6] indicated a set of suitable textural features for sandstone characterization. The results from the current experiment have shown quite different results. A data set of 11 samples is still very small, however, we believe that the results in this report are more representative and general.

The experiments in [6] indicated that layering in sandstone facies could be a problem when applying textural features to characterize the sandstone. It has been demonstrated here that the layering can be suppressed by a method suppressing large-scale spatial features in an image. The method removes most of these features without affecting the textural contents of the image. The method could probably be optimized more by performing an experiment on a larger data set of layered sandstone facies.

The textural experiments indicated that some of the textural features show strong correlation with the sandstone parameters. Strongest correlation was found for the Local GLCM features Inertia and Contrast, and the Global GLCM features Inverse Difference Moment and Intertia. The strongest correlation were found between grain size and Inertia (95%).

Some geometrical features were extracted from segmented sandstone images. These features were tested on both the previous data set [6] and the current data set. Very strong correlations were found between quartz and mean region size, and porosity and mean region size. However, the correlation was not very high for any of the geometrical features derived from the current data set.

Linear regression models based on the best Global and Local GLCM textural measures were calculated for the sandstone parameters. These models were applied for prediction of the parameters for samples no. 3, 8, 11, 14, and 16. Table 14 shows the results.

No.	Permeability	Porosity	Grain size	Quartz	Clay	Feldspar
3	1.92	18.20	0.16	51.9	20.5	23.6
8	0.73	18.34	0.11	51.1	20.2	23.1
11	1.10	18.48	0.13	53.2	19.8	23.8
14	1077	22.60	0.36	77.4	10.1	15.0
16	0.19	15.37	0.09	43.5	27.2	23.6

Table 14: *Predicted parameter values for samples no. 3, 8, 11, 14, and 16 in the image mosaic.*

Predictions were also calculated using PLS regression on a subset of the GLCM spectra (see [7] for more on PLS regression). This work was done by the SINTEF group and reported by them. The results are similar to that of Table 14.

The physical measurements of the sandstone parameters were released from ResLab A/S at

No.	Permeability	Porosity	Grain size	Quartz	Clay	Feldspar
3	5.02	20.5	0.17	65	13	22
8	0.819	15.6	0.08	43	32	23
11	0.747	15.9	0.14	48	27	25
14	2050	23.3	0.34	82	6	12
16	0.428	15.0	0.08	49	26	22

Table 15: *Sandstone parameters measured physically by ResLab A/S.*

the time of closing the work on this report. The values are given in Table 15. A comparison of the predicted values and the physically measured values indicates very encouraging results.

In conclusion, the experiment has demonstrated that it should be possible to predict several of the sandstone parameters using textural features. A larger data set is needed to say more about the accuracy which can be expected in an operational situation.

References

[1] F. Albregtsen, "Detection of Cancer by 2-D Texture Analysis of Liver Cell Nuclei", Presented at the NORSIG conference, Norway October 25-26, 1990.

[2] R. Andrle, "The Angle Measure Technique: A New Method for Characterizing the Complexity of Geomorphics", Journal of Mathematical Geology, 1994, pp. 83-97.

[3] R.W. Conners, M.M. Trivedi and C.A. Harlow, "Segmentation of a High-Resolution Urban Scene Using Texture Operators", *Computer Vision, Graphics, and Image Processing*, vol. 25, pp. 273-310, 1984.

[4] R.C. Gonzalez and P. Wintz, *Digital Image Processing*, 2nd edition, Addison-Wesley, 1987.

[5] R. Haralick, K. Shanmugam and I. Dinstein, "Textural Features for Image Classification", *IEEE Transactions on Systems, Man, and Cybernetics*, vol. SMC-3, No. 6, p. 610-621, November 1973.

[6] H. Koren, A.H.S. Solberg, O.M. Halck, and R. Solberg, *Texture analysis of sandstone surfaces*, NR Note BILD/08/94, Norwegian Computing Center, Oslo, August 1994.

[7] Martens and Ness, *Multivariate Calibration*, Wiley, 1989.